Influence of Molecular Weight on Phase Transitions and Alignment of a Thermotropic Nematic Polyester

Rita B. Blumstein,* Eleanor M. Stickles, Michelle M. Gauthier, and Alexandre Blumstein

Polymer Science Program, Department of Chemistry, University of Lowell, Lowell, Massachusetts 01854

Ferdinand Volino

Groupe de Physico-Chimie Moleculaire, Physique du Solide, DRF-CENG, 85X, 38041 Grenoble Cedex, France. *Received February 23, 1983*

ABSTRACT: We have investigated oligomers, polymers, and a model of poly(4,4′-dioxy-2,2′-dimethylazoxybenzenedodecanedioyl). The molecular weights ranged from approximately 700 to 19000. In the oligomeric range, the kinetics of melt and cold crystallization, as well as the kinetics of macroscopic sample alignment in a magnetic field of ~1.8 T, is controlled by the aromatic end-group distribution. Phase transition temperatures increase with increasing molecular weight. A biphasic region (nematic + isotropic) is observed for all oligomers and polymers. Its range of thermal stability shrinks from ~40 to ~5 °C as the molecular weight increases. The value of the glass transition temperature is nearly independent of molecular weight or development of crystallinity. The values of phase transition entropy at the N → I transition and of the nematic order parameter increase with increasing molecular weight to reach a plateau at average chain lengths of 8–10 repeating units. Development of a polymeric mesophase, as characterized by maximum local chain extension, appears to require cooperativity between 8–10 repeating units per chain. The semicrystalline state of higher molecular weight samples is represented in terms of a fringed micelle model, with extended-chain segments forming cybotactic nematic domains.

Introduction

We have recently prepared a series of thermotropic nematic polyesters in which substituted azoxybenzene mesogens

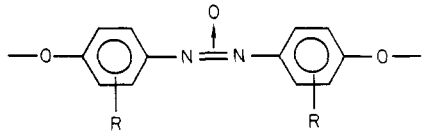

regularly alternate with flexible alkanedioyl spacer moieties $-OC(CH_2)_nCO-$.[1-3] Structure broadening by lateral substitution of the aromatic core results in formation of highly soluble polymers with moderate to low transition temperatures and a nematic thermal stability range of about 15–75 °C for homopolymers and up to 150 °C for copolymers.

We have investigated in some detail the series of polymers

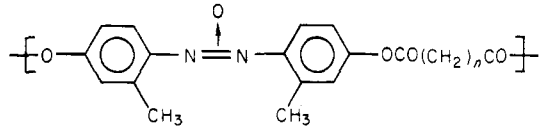

formed by condensation of 4,4′-dihydroxy-2,2′-dimethylazoxybenzene (mesogen 9) with the diacid chlorides $ClCO(CH_2)_nCOCl$. In the range of spacer lengths studied (values of n up to 14), the polymers are characterized by high values of isotropization enthalpies ΔH_{NI}, compared with low molecular weight nematics, and strong, persistent odd–even oscillation of T_{NI} and ΔH_{NI}.[3] This indicates participation of the spacer in the ordering process upon transition to the mesophase. The I → N phase transition, as investigated by measurement of magnetic birefringence, is indeed characterized by drastic intramolecular conformational changes from randomly coiled chains to chains with a high degree of alignment.[4,5]

For poly(4,4′-dioxy-2,2′-dimethylazoxybenzenedodecanedioyl), the high degree of local chain extension has been confirmed by proton magnetic resonance and X-ray diffraction studies. This polymer is designated as DDA-9 (IUPAC name: poly[oxy(3-methyl-1,4-phenylene)azoxy(2-methyl-1,4-phenylene)oxy(1,12-dioxo-1,12-dodecanediyl)]). The order parameter of a macroscopically oriented nematic phase of DDA-9 is unusually high compared to that of classical nematics, especially in the vicinity of the I → N transition; moreover, we have found that the same degree of order is required for both spacer and mesogen if satisfactory agreement between experimental and simulated spectra is to be achieved.[6,7] The X-ray diffractogram of a quenched aligned nematic DDA-9 also shows extension of the spacer and a picture very similar to that of the oriented low molecular weight *n*-alkoxyazoxybenzenes, with two diffuse equatorial peaks and four sharp inner peaks at 50° from the meridian corresponding to the fiber period.[2] This suggests that the organization of the nematic phase of DDA-9 can be interpreted in terms of the cybotactic nematic model proposed by de Vries.[8]

Model compounds of polymer DDA-9 are not mesomorphic. Structures such as

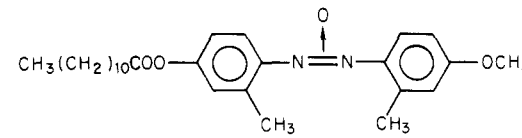

a model of the repeating unit with its flexible–rigid sequence, or prepolymer

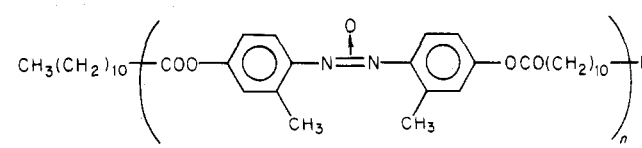

DDA-9-DDA-9-DDA
$n = 2$; R = CH_3

do not display liquid crystalline behavior.[9] Approximately 5–6 repeating units per chain are required for the appearance of an enantiotropic nematic phase, though a monotropic mesophase (i.e., nematic on cooling only) is observed at lower molecular weights when a rigid–flexi-

0024-9297/84/2217-0177$01.50/0

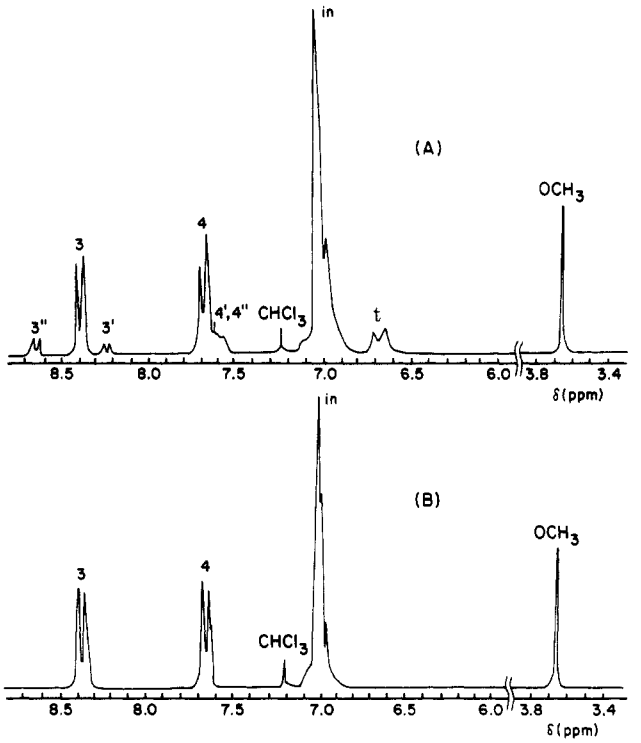

Figure 1. High-resolution NMR spectra of terminal groups. (A) Terminal 9 and terminal DDA moieties are present. (B) Only terminal DDA moieties are present. Peak assignments are as described in the Experimental Section.

ble–rigid sequence without flexible tails is produced as in the model

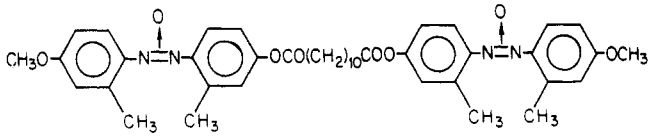

9-DDA-9

As part of a continuing investigation of the influence of molecular weight on the properties of DDA-9 we present here the results of phase transition and alignment studies of a series of samples ranging in molecular weight from about 700 to 19 000. Polarizing microscopy, differential scanning calorimetry, and high-resolution and wide-line proton NMR were used as tools for sample characterization.

Experimental Section

Monomers and samples T, SP, L, and M6 were prepared by interfacial polycondensation as described in ref 1. Synthesis and characterization of model compounds were as in ref 9. The remaining samples were prepared by room-temperature solution polymerization under anhydrous conditions. Unreacted acid chloride end groups were converted to $-COOCH_3$. In the oligomeric range, the stoichiometric ratio of mesogen 9 to $ClCO-(CH_2)_{10}COCl$ was adjusted to yield approximately the desired molecular weight.

Molecular weights of samples with $\bar{M}_n > \sim 7000$ were measured as in ref 2. Molecular weights of the remaining samples were determined by end-group titration using ^1H NMR spectroscopy. The samples were dissolved in chloroform (~2% by weight), and the spectra were recorded with a Bruker WM-250 instrument operating at 250 MHz. The aliphatic chain ends were assumed to be quantitatively converted to the methyl ester. Tests for chlorine were indeed negative; the amounts of carboxylic acid end groups, if any were present, were too small for reliable potentiometric titration, and their presence was neglected. The aliphatic end groups (terminal DDA) were titrated by measuring the OCH_3 peak area at δ 3.67 (see Figure 1).

Assignments of chemical shifts corresponding to the aromatic end groups (terminal 9) are as in Figure 1 and were made by comparing spectra of polymers and model compounds. For polymers (negligible end-group contribution) the assignments are as follows:

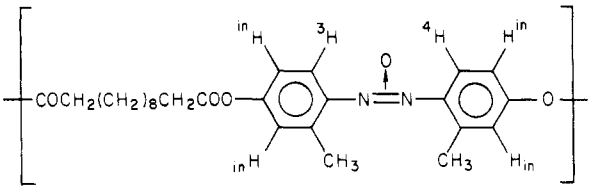

For symmetrically substituted mesogen 9 we have

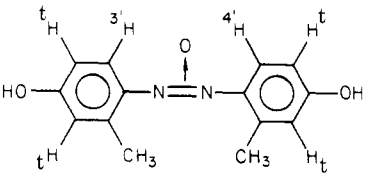

An unsymmetrically substituted model (or a terminal 9 moiety) contains internal (in) and terminal (t) peaks in a mixture of structural isomers as in

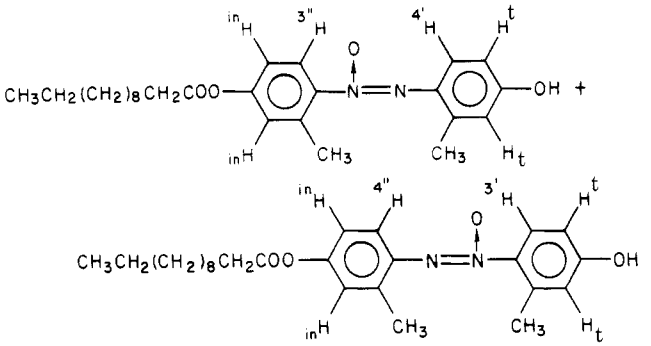

Thermal analysis was performed with a Perkin-Elmer DSC2C differential scanning calorimeter calibrated in the usual manner. In order to provide a consistent thermal history, each material studied was first heated to at least 20 °C above the crystal-to-isotropic (K → I) or nematic-to-isotropic (N → I) transition. DSC traces were obtained by cycling the sample betwen that temperature and 240 K. Except for the first heating scans, all DSC traces were completely reproducible from cycle to cycle. The heating and cooling rates were 10 °C/min.

Textures of the materials were studied with a Leitz Ortholux polarizing microscope equipped with a hot stage and a Mettler FP-52 temperature programmer.

Wide-line ^1H NMR spectra were obtained by using a Bruker CXP-100 pulsed spectrometer operating at ~75 MHz, with a spectral width of 125 kHz. The samples were heated to the isotropic state and then cooled by steps of 1–5 °C, with about a 10-min residence time at each temperature before recording of the spectra. Order parameters were deduced from dipolar splittings as in ref 7. Experimental conditions were improved relative to those of ref 7 due to shorter dead time in recording free induction decay (FID) signals, yielding more exact line shapes after fast Fourier transform.

Results and Discussion

The number-average molecular weights and ratios R of aromatic to aliphatic end groups of some representative samples with values of $\bar{M}_n < \sim 5000$ are listed in Table I. The value of $\bar{M}_n$ was calculated by setting $\overline{DP}$, the number of repeating units per chain, as in eq 1 or 1′.

$$\overline{DP} = [(\text{area}_{\text{tot aromatic}}/6) + (\text{area}_{-(CH_2)_8-}/16)]/[(0.5 \times \text{area}_{\text{tot}}) + (0.333 \times \text{area}_{-OCH_3})] \quad (1)$$

$$\overline{DP} = \left[2 \times \frac{(\text{area}_{\text{tot aromatic}}/6)}{(0.5 \times \text{area}_{\text{tot}})} \times N_{[9\text{-DDA}]_x\text{-}9} \right] + \left[\frac{(\text{area}_{\text{tot aromatic}}/6)}{(0.5 \times \text{area}_{\text{tot}})} \times N_{[9\text{-DDA}]_x} \right] \quad (1')$$

Weighting factors $N_{[DDA\text{-}9]_x\text{-}DDA}$, $N_{[9\text{-DDA}]_x\text{-}9}$, and $N_{[9\text{-DDA}]_x}$ were calculated from end-group ratios by neglecting species in which both ends would be contributed by the underrepresented terminal group.

Samples J and E were among fractions obtained by nonsolvent precipitation from an initial oligomer prepared with excess monomer 9. Sample J is nearly monodisperse (1 major and 2 minor spots on TLC); E was further split by column chromatography, with separation occurring largely by end-group type due to preferential adsorption of monomer 9 end groups (EI and EII are listed). Initially, unfractionated L was similarly split on a chromatographic column (LI, LII, and LIII are listed). The remaining samples were not fractionated.

In Table II are listed the phase transitions observed by polarizing microscopy upon heating. A homogeneous fluid nematic phase is observed between T_N and T_2, and the last trace of birefringence disappears at the clearing temperature T_c. Nematic and isotropic phases coexist between T_2 and T_c (N + I biphasic region). Phase transition temperatures increase with increasing molecular weight. Stability of the N + I biphase observed upon heating shrinks to a few degrees for the highest molecular weights. Temperature T_c is typically supercooled by 10–15 K in all but the highest molecular weight samples. Supercooling of T_2, on the other hand, does not exceed a few degrees, which results in narrowing of the biphasic range observed on cooling. Homogeneous nematic textures can be preserved down to room temperature in some samples. In others, onset of crystallization on cooling can be visually observed in a range of temperatures roughly corresponding to that at which "transition" spectra are recorded by wide-line ^{1}H NMR (see below). All samples eventually develop some crystallinity upon standing at room temperature.

Table III shows phase transitions as recorded by DSC upon heating and cooling. Only data relative to second and/or subsequent heating cycles are reported. Figure 2 illustrates three typical thermograms. Figure 2A is representative of samples with $\bar{M}_n \geq \sim 5000$ and $R \sim 1$. It shows the standard mesophase behavior with K → N and N → I transitions on heating and cooling. As is usual in mesophase polymers, supercooling of T_{IN} is moderate. The N → K transition is supercooled by ~30 K. A small cold crystallization exotherm is occasionally observed at T_{NK} on heating the solid phase above its nematic glass transition temperature T_g. A reproducible premelting process is followed by recrystallization. Figure 2B is representative of samples with $\bar{M}_n \leq \sim 5000$ and 9/DDA end-group ratios $\leq \sim 3.5$. Most, if not all, crystallization process occurs as cold crystallization at T_{NK} on heating, followed by a premelting zone similar to that of Figure 2A. For sample DDA-9-L, X-ray diffractograms show that the sharpest crystalline structure develops ~85 °C following premelting. Behavior of samples with $\bar{M}_n \leq \sim 5000$ and aromatic/aliphatic end-group ratios $\geq \sim 3.5$ is illustrated in Figure 2C. These samples are characterized by the absence of crystallization under the scanning conditions reported here. Sample M3 shows a transitional DSC scan, with a modest crystallization peak from the nematic melt at T_{NK} on cooling. All samples eventually develop some crystallinity upon annealing.

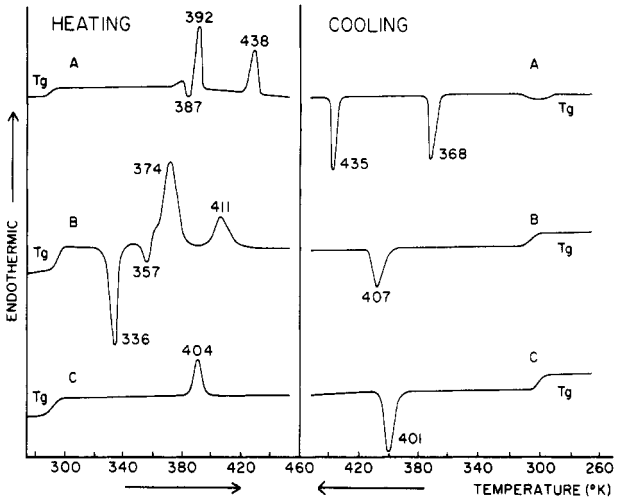

Figure 2. DSC scans of representative samples: (A) sample T2 ($R \sim 1$, $\bar{M}_n = 18700$); (B) sample L ($R = 1.5$, $\bar{M}_n = 4000$); (C) sample E ($R = 8.5$, $\bar{M}_n = 3200$). Transition temperatures in K.

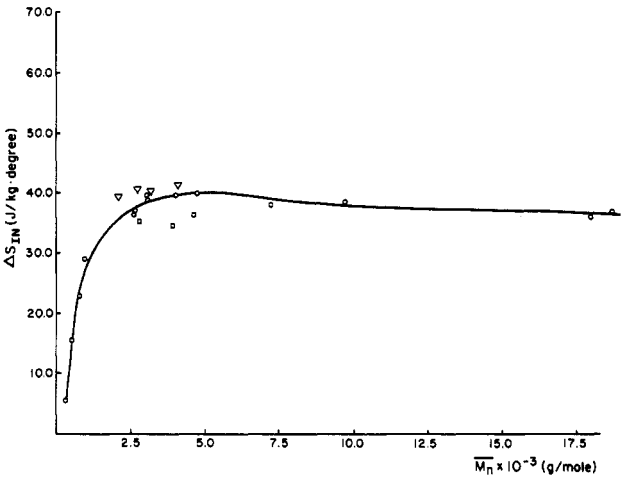

Figure 3. Isotropic → nematic transition entropies as a function of molecular weight. First four points refer to PAA, DAB, model 9–DDA–9, and oligomer J, in that order. For remaining points, triangles represent samples with values of $R > 5$; squares, $R < 1$; and circles, intermediate values of R.

It would seem that crystallization kinetics is end-group controlled, with cold crystallization nucleated above a critical concentration of aliphatic chain ends.

Stability of the mesophase seems to be reduced by DDA end groups, as illustrated by comparison of phase transition temperatures of samples M4 ($R = 0/1$), M5 ($R = 0/1$), L ($R = 1.5/1$), LII ($R = 1.5/1$), and M3 ($R = 1/0$), all of which have comparable molecular weights.

We should also point out that the lowest molecular weight to display an enantiotropic nematic phase is that of sample M1 ($\overline{DP} \sim 5$), which is almost exclusively 9-terminated; DDA-terminated oligomers in this range of molecular weight are not mesomorphic.

The nematic glass transition temperature T_g, which was measured as the point of inflection on heating (Table III and Figure 2), is remarkably independent of molecular weight. There appears to be a slight dependence on end-group ratio, with a small decrease in T_g for values of $R \ll 1$. Development of crystallinity does not increase the value of T_g. The crystalline fraction W_C was measured for a sample of $\bar{M}_n \sim 11000$[10] and found to be ~0.5; samples SP, M6, T1, and T2 develop a comparable degree of crystallinity upon cooling from the nematic melt. The remaining samples are either noncrystalline (supercooled nematic glass) or weakly crystalline below T_g.

Table I
Characterization of Samples by End-Group Analysis

sample	$\bar{M}_n$	R^a	weighting factor $N_{[9\text{-DDA}]_x\text{-}9}$	weighting factor $N_{[9\text{-DDA}]_x}$	weighting factor $N_{[\text{DDA-9}]_x\text{-DDA}}$
J	900	9.2/1.0	0.80	0.20	
EI	2600	4.0/1.0	0.60	0.40	
EII	3000	4.9/1.0	0.66	0.34	
E	3200	8.5/1.0	0.78	0.22	
LI	2800	0.85/1.0		0.92	0.08
LII	4800	1.5/1.0	0.20	0.80	
LIII	3000	3.2/1.0	0.52	0.48	
L	4000	1.5/1.0	0.20	0.80	
M1	2200	9.8/1.0	0.82	0.18	
M2	2600	2.7/1.0	0.46	0.54	
M4	4700	0.0/1.0			1.00
M5	4000	0.0/1.0			1.00
M3	4200	1.0/0.0	1.00		

[a] Ratio of aromatic to aliphatic end groups (9/DDA).

Table II
Phase Transitions Observed by Polarizing Microscopy[a]

sample	$\bar{M}_n$	T_N[b]	T_2[b]	T_c[b]
DDA-9-J[c]	900	No mesophase on heating		
-EI	2,600	376.8	384.8	426
-EII	3,000	370.8	401.0	430.8
-E	3,200	360	398	412
-LI	2,800	379.2	394.5	422.6
-LII	4,800	377.5	401.1	423.7
-LIII	3,300	375.4	404.9	419.9
-L	4,000	377.6	408.5	423.7
-M1	2,200	364	385	395.7
-M2	2,600	361.5	399	409
-M3	4,200	376.8	409.4	423.6
-M4	4,700	385	401.5	426
-M6	7,200	391.8	420.7	440.5
-T1	18,000	393	435	442

[a] Heating rate = 10 °C/min. [b] In K. [c] Monotropic nematic (on cooling: T_c = 353 K; T_2 = 323 K).

On Figure 3 are plotted the values of isotropization entropies as a function of molecular weight. They were measured on cooling as described in ref 11. Three model compounds are included: 4,4′-dimethoxyazoxybenzene (PAA), 4,4′-bis(decyloxy)azoxybenzene (DAB), and model 9–DDA–9. The data for PAA and DAB are taken from ref 12, as the corresponding derivatives of mesogen 9 are not mesomorphic. Beginning with the values of ΔS_{IN} for PAA and DAB, which are within the usual range found for low molecular weight nematics, the isotropization entropy increases drastically for the two monotropic samples, model 9–DDA–9 and oligomer DDA–9-J. The values of ΔH_{IN} and ΔS_{IN} continue to increase through the oligomeric range to reach a maximum of ~16 kJ/kg and ~40 J/(kg·K), respectively.

At the N → I transition the enthalpy change is primarily intramolecular and results partly from conformational changes in the flexible spacer moiety. The results of Figure 3 indicate that, in the oligomers, cooperativity between repeating units brings about increasing extension of the spacer in the nematic phase as the molecular weight increases.

For the DDA–9 system we can define a polymer as a molecule sufficiently long to allow maximum degree of local chain extension to develop. The point at which this transition occurs appears to depend to some extent on the type of end groups present. (End capping with aliphatic DDA groups seems to decrease ordering of the mesophase.) In order to delineate the transition to a polymeric behavior, we have investigated order parameters and sample alignment in the magnetic field of our NMR spectrometer (~18 kG) as a function of molecular weight. The following samples were studied: monotropic model compound 9–DDA–9, monotropic DDA–9-J, and enantiotropic DDA–9-E, -L, and -LII.

Representative spectra are illustrated in parts 4A–F of Figure 4, which show (A) an isotropic phase, (B) a N + I

Table III
Phase Transitions As Determined by DSC[a]

sample	$\bar{M}_n$	heating T_g	heating T_{NK}	heating T_{KN}[b]	heating T_{NI}	cooling T_{IN}	cooling T_{NK}
J[c]	900	282				347	
M1	2200	283			383	377.5	
EI	2600	285			403	400	
M7	2800	282			393	390	
EII	3000	286			404.5	401	
E	3200	282			404	401	
M3	4200	284		374.5	411	406	~338
M2	2600	282	320 (b)[d]	357	398	394	
LI	2800	280	325	374	404	401	~329
LIII	3300	284	339	373	410	407	
L	4000	282	336	374	411	405	
LII	4800	283	339	374	411	406	~338 (b)[d]
M5	4000	277	363	378	400	398	347
M4	4700	277	366	382	407	399	346
M6	7200	278	370	389	424	417	344
SP	9700	280		394	432	427	366
T1	18000	281		394	437	433	360
T2	18700	281		392	438	435	368

[a] In K; scanning rates: 10 °C/min. [b] Main-peak maximum. [c] No mesophase on heating (T_{KI} = 355). [d] b = broad peak.

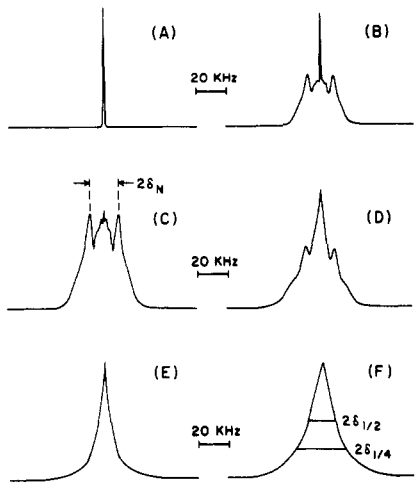

Figure 4. Some representative PMR line shapes (sample LII on cooling): (A) isotropic phase at 147 °C; (B) N + I biphase at 129 °C; (C) macroscopically aligned nematic phase at 110 °C; (D) transition spectrum recorded at 85 °C; (E) solid phase at 78 °C; (F) solid phase at 40 °C.

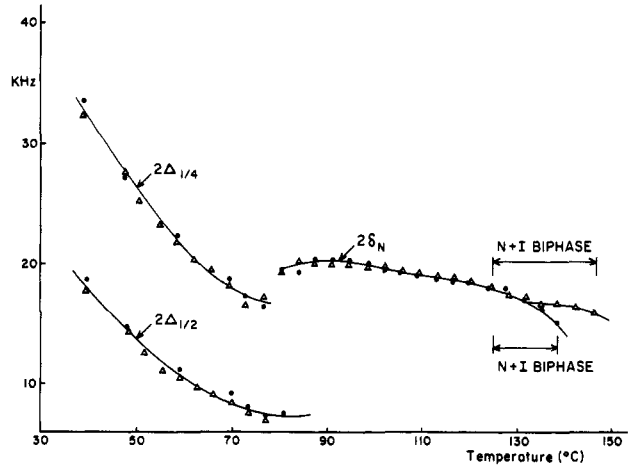

Figure 5. Spacings $2\delta_N$ and line widths at quarter- and half-height as a function of temperature on cooling. Triangles represent sample L; circles represent sample LII. Temperatures reported in °C.

biphase, (C) a pure nematic phase homogeneously aligned, (D) a transition spectrum, and (E, F) solid spectra.

Examination of line shapes reveals the presence of biphasic regions above and below the temperature range of the homogeneously aligned nematic phase. The fraction of aligned nematic phase, f_N, present in the N + I biphase was measured from the FID signals, where contributions of aligned nematic and isotropic phases are well separated. The order parameter S associated with the mesogenic moiety was calculated from the $2\delta_N$ spacings (see Figure 4C) as described previously. Crystallization from the melt destroys macroscopic sample alignment. This is illustrated in Figure 5, which shows a plot of spacings $2\delta_N$ (proportional to S) and line widths at quarter- and half-height ($2\Delta_{1/4}$ and $2\Delta_{1/2}$) for samples DDA-9-L and DDA-9-LII. In the range of temperatures corresponding to the transition spectra (Figure 4D), which correlates roughly with the onset of crystallization observed by polarizing microscopy, the nematic order parameter appears to decrease. Upon passage to the solid state, macroscopic alignment is destroyed, as evidenced by line shape change and drastic decrease in line width.

Comparison of the NMR behavior of samples L and LII is instructive (Figure 5). Sample LII is a fraction obtained

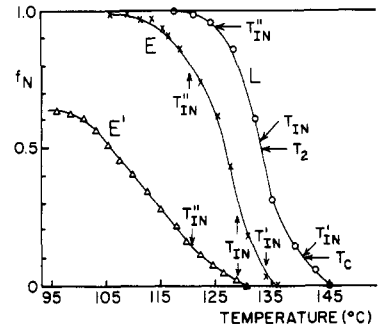

Figure 6. Fraction of aligned nematic phase as a function of temperature (on cooling from the isotropic phase as described in the Experimental Section): (L) sample L heated ~5 °C into the isotropic phase; (E') sample E heated ~5 °C into the isotropic phase; (E) complete alignment of sample E after heating to ~20 °C into the isotropic phase. T_{IN} is the DSC peak maximum; T'_{IN} and T''_{IN} are measured at the high- and low-temperature end of the DSC transition, respectively. Biphase observed by microscopy between T_c and T_2.

by chromatographic separation from L; it has the same end-group ratio as L but comparison of molecular weight distributions reveals that it lacks the longest and shortest molecules initially present in L. Removal of the longest molecules is reflected in the values of $2\delta_N$ in the N + I biphase and the narrowing of this region. At a given temperature in the biphase the order parameter is lower for LII than for L. These results seem to indicate that upon cooling from the isotropic phase the molecules align sequentially, with the longest species aligning first and, in the biphase, more efficiently. In the homogeneously aligned nematic phase both samples have approximately the same degree of order. (The undulations in the plot of $2\delta_N$ vs. temperature do not seem to be an artifact and will be discussed elsewhere.)

The highest molecular weights (DDA-9-T1, for example) do not align in the field of the spectrometer, so that the K → N transition on heating is characterized by discontinuity in line width without change in line shape. A shape similar to that of Figure 4E is found on both sides of the transition. This suggests that the unoriented semicrystalline solid has a structural organization with local chain extension similar to that of the aligned nematic phase, except for domain size. Starting with this assumption, we have indeed been able to simulate the experimental solid-phase spectra of DDA-9-L (Figure 4E,F) from the corresponding spectrum of the oriented nematic phase (Figure 4C). It would appear, then, that crystallization from the melt occurs in the extended-chain conformation. The semicrystalline solid state could perhaps be modeled by a fringed micelle in which cybotactic nematic domains[2,8] of extended-chain segments replace the traditional amorphous component. This nematic noncrystalline component would be relatively ordered, and one would not expect in the NMR spectrum the narrow line of ~0.1 G usually associated above T_g with a "mobile" noncrystalline fraction. This is confirmed experimentally and could be an explanation of the lack of dependence of T_g on molecular weight and crystallnity.

The fraction f_N of aligned nematic obtained on cooling from the isotropic phase is shown in Figure 6 for samples L and E. When heated to the isotropic state and then cooled as described in the Experimental Section, samples L and LII aligned completely below the I → N transition, but samples E, J, and 9-DDA-9 did not. Complete alignment of these samples was achieved after heating to a temperature ~20 °C above the K → I (J and 9-DDA-9) or N → I (E) transition. As E, J, and 9-DDA-9 are pre-

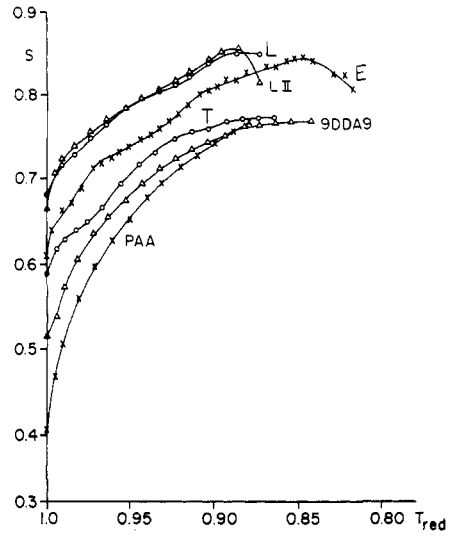

Figure 7. Order parameters as a function of molecular weight. T_{red} is an arbitrary temperature defined as $T_{red} = T/T_{IN}$.

dominantly or completely terminated by aromatic groups, while L and LII contain a relatively high proportion of terminal DDA units, it would seem that the kinetics of macroscopic alignment in the nematic phase is controlled by aromatic chain ends.

It is clear from Figure 6 that the experimentally determined I → N transition temperature depends on the method of observation. As a first approximation we assume that the N + I biphase is bracketed by temperatures T'_{IN} and T''_{IN} obtained by extrapolation to the base line at each end of the I → N transition recorded by DSC. In this biphasic region the order parameter S increases rapidly with decreasing temperature, indicating that the nematic alignment is strongly perturbed by the presence of an isotropic component. On Figure 7 are plotted the values of S as a function of an arbitrary reduced temperature $T_{red} = T/T_{IN}$, where T_{IN} is the DSC peak maximum observed on cooling. This temperature corresponds to values of $f_N \sim 0.5$–0.8. For comparison, we have also plotted the values of S for PAA, a classical low molecular weight nematic; these values were calculated from data listed in ref 13 and with $T_{red} = T/T_c$, where T_c is the thermodynamic clearing temperature. The values of S increase with increasing molecular weight and appear to reach a limit at sample L. For samples L and LII the order parameter reaches a maximum value of $S \sim 0.85$, before destruction of nematic alignment by incipient crystallization. It is interesting to note that the maximum value of S for supercooled nematic PAA, 9–DDA–9, and J is $S_{max} = 0.76$ (for sample J the uncertainty is 0.76 ± 0.02). On the basis of the data of Figure 7 it would appear that the maximum degree of ordering is developed for an average chain length of 8–10 repeating units. At temperatures T''_{IN} the values of S are ~0.75 for L and LII. This represents the upper limit of the order parameters predicted by Ronca and Yoon[14] for the isotropic–nematic transition of semiflexible polymers in the limit of high molecular weights. However, meaningful comparison with theoretical predictions cannot be made at this point because the value of the thermodynamic I → N transition temperature is uncertain. Further experimentation with narrow fractions is clearly required.

Conclusion

We have investigated phase transitions of a series of samples ranging in molecular weight from about 700 to 19 000. Phase transition temperatures increase with increasing molecular weight. For unfractionated samples with roughly balanced end-group ratios the molecular weight can be calculated from the equation

$$\frac{1}{T_{NI}} = \frac{1}{445.8} + \frac{1.758 \times 10^{-3}}{\overline{DP}}$$

(obtained from a fit of 11 data points).

Because of end-group and molecular weight distribution we are dealing with multicomponent systems so that a N + I biphase is observed. The stability range of this biphase is erratic at first, probably due to heterogeneity of distributions from sample to sample; it eventually shrinks to a few degrees as the relative contribution of chains with $T_{NI} < (T_{NI})_{limiting}$ is decreased. The sequential alignment of chain lengths in the biphasic region of samples L and LII reflects selective transferral of the longest species to the anisotropic phase, in qualitative agreement with theory.[15] Phase equilibria of mixtures of monodisperse systems will be established before further discussion of this point is considered.

Kinetics of macroscopic alignment of the nematic phase of oligomers in the magnetic field appears to be governed by the distribution of rigid end groups. By varying the thermal history of model 9–DDA–9, for example, we have found values of f_N ranging from insignificant to 1.0 below the temperature of the I → N transition. Similarly, kinetics of melt and cold crystallization appears to be controlled by the distribution of end groups. In the range of samples investigated, values of glass transition temperatures do not increase with molecular weight or development of crystallinity. This result, together with the conclusions drawn from investigation of NMR line shapes, suggests that the semicrystalline solid state might be represented by a fringed micelle with extended-chain cybotactic nematic domains. This is in agreement with the cytobactic nematic model previously proposed for quenched nematic glass of DDA–9.[2]

Crystallization from the oriented nematic melt, though appearing to occur in extended-chain conformation, destroys macroscopic sample alignment. This has been observed even upon slow cooling in a magnetic field as high as 12 T.[5]

Development of a polymeric mesophase, as characterized by a high degree of local chain extension, appears to require cooperativity between approximately 8–10 repeating units per chain.

Acknowledgment. We are indebted to Mr. O. Thomas and Dr. S. Ponrathnam for preparation of the high molecular weight samples. This work was supported in part by NSF Grant DMR-7927059 and NSF Equipment Grant DMR-8108697. The high-resolution NMR work was carried out at the Worcester Consortium NMR Facility.

References and Notes

(1) A. Blumstein and S. Vilasagar, *Mol. Cryst. Liq. Cryst., Lett.*, **72**, 1 (1981).
(2) A. Blumstein, S. Vilasagar, S. Ponrathnam, S. B. Clough, G. Maret, and R. B. Blumstein, J. *Polym. Sci., Polym. Phys. Ed.*, **20**, 877 (1982).
(3) A. Blumstein and O. Thomas, *Macromolecules*, **15**, 1264 (1982).
(4) A. Blumstein, G. Maret, and S. Vilasagar, *Macromolecules*, **14**, 1543 (1981).
(5) G. Maret and A. Blumstein, *Mol. Cryst. Liq. Cryst.*, **88**, 295 (1982).
(6) F. Volino, A. F. Martins, R. B. Blumstein, and A. Blumstein, *C. R. Hebd. Seances Acad. Sci., Ser. B*, **292**, 829 (1981); *J. Phys. (Paris) Lett.*, **42**, L305 (1981).
(7) A. F. Martins, J. B. Ferreira, F. Volino, A. Blumstein, and R. B. Blumstein, *Macromolecules*, **16**, 279 (1983).
(8) A. de Vries, *Mol. Cryst. Liq. Cryst.*, **10**, 219 (1970).

(9) R. B. Blumstein and E. Stickles, *Mol. Cryst. Liq. Cryst., Lett.*, **82**, 151 (1982).
(10) J. Grebowicz and B. Wunderlich, *J. Polym. Sci., Polym. Phys. Ed.*, **21**, 141 (1983).
(11) R. B. Blumstein, E. Stickles, and A. Blumstein, *Mol. Cryst. Liq. Cryst. Lett.*, **82**, 6, 205 (1982).
(12) H. Arnold, *J. Phys. Chem.*, **226**, 146 (1964).
(13) E. G. Hanson and Y. R. Shen, *Mol. Cryst. Liq. Cryst.*, **36**, 193 (1976).
(14) G. Ronca and D. Y. Yoon, *J. Chem. Phys.*, **76**, 3295 (1982).
(15) P. J. Flory and R. S. Frost, *Macromolecules*, **11**, 1126 (1978). P. J. Flory, *Ber. Bunsenges. Phys. Chem.*, **1981**, 885 (1977).

Phase Equilibria and Transition in Mixtures of a Homopolymer and a Block Copolymer. 1. Small-Angle X-ray Scattering Study

Wang-Cheol Zin and Ryong-Joon Roe*

Department of Materials Science and Metallurgical Engineering, University of Cincinnati, Cincinnati, Ohio 45221. *Received March 17, 1983*

ABSTRACT: The small-angle X-ray scattering technique is utilized to study the phase separation and phase transition occurring in mixtures of a styrene–butadiene diblock copolymer with a low molecular weight polystyrene. At low temperatures the scattering curve shows a main peak and a secondary peak, indicating the presence of well-developed microdomains. As the temperature is raised the peaks gradually lose intensity. The binodal and spinodal temperatures for the transition between the ordered structure at low temperature and the disordered, homogeneous structure at high temperature are determined and found to increase with increasing amount of added polystyrene. At low temperatures, with increasing amount of polystyrene, the main peak at first shifts toward lower angles, indicating an increased distance between microdomains. However, at concentrations beyond about 50% polystyrene, which evidently corresponds to the solubility limit of the latter in the microdomains, the peak position remains constant. The observed shift in the relative position of the secondary peak suggests that the morphology of the microdomains changes gradually from spherical to lamellar as the proportion of polystyrene is increased. With all the mixtures no evidence is found for an increase in the microdomain boundary thickness with increasing temperature.

I. Introduction

Block copolymers often attain geometrically regular arrangements of microdomains consisting of components segregated from eath other. On heating, such a block copolymer can sometimes be transformed into a homogeneous, disordered structure. The temperature of the transition depends on the degree of compatibility of the components forming the blocks and the lengths of the blocks. The presence of a diluent such as a common solvent or a compatible polymer also influences the transition temperature. In recent years a number of workers made theoretical and experimental studies that touch upon the transition phenomenon of block copolymer systems. To cite a few examples, Leibler[1] developed a theory that predicts the transition temperature. Chung and Gale[2] and Gouinlock and Porter[3] found a discontinuity, on changing the temperature, in the rheological properties of a styrene–butadiene triblock copolymer. We[4] made a detailed study of the effect of temperature on the small-angle X-ray scattering from styrene–butadiene diblock and triblock copolymers and obtained evidence of transition from a ordered, microdomain structure to a disordered, homogeneous structure.

In this work we extend the previous small-angle X-ray scattering study[4] to investigate mixtures of a styrene–butadiene diblock copolymer with various proportions of a low molecular weight polystyrene. We are interested in finding out how the addition of the homopolymer alters the structure of the microdomains and the temperature of transition to the disordered structure. We are also interested in determining the limit of solubility of the polystyrene in the microdomains of the block copolymer. In the companion paper,[5] we report on the results of cloud point measurements on the same mixture system and also on two other similar systems containing the styrene–butadiene block copolymer and either a polystyrene or a polybutadiene. Combining the results of the present small-angle X-ray scattering studies with those of the cloud point measurements, we have been able to construct phase diagrams[5] of such mixtures. They exhibit fascinating interplays of the phase separation behavior with the transition of the block copolymer between the ordered and disordered structures.

II. Experimental Section

A. Materials. The polystyrene homopolymer was purchased from Pressure Chemical Co., and its M_n (by vapor phase osmometry) and M_w (by viscometry) are 2200 and 2400, respectively, according to the information provided by the supplier. The styrene–butadiene diblock copolymer contains approximately 25% styrene and was kindly synthesized for our use by Dr. H. L. Hsieh of Phillips Petroleum Co. According to Dr. Hsieh, its M_n and M_w (by GPC) are 27 000 and 28 000, respectively, and the microstructure of the butadiene blocks (by IR) is 30% vinyl, 42% trans 1,4, and 28% cis 1,4. The styrene content was determined by the NMR technique in this laboratory[6] and found to be 27 ± 1%. This polymer was also characterized independently by Krause et al.[7] by NMR and GPC.

The polystyrene and the styrene–butadiene diblock copolymer are the same materials used in our previous study,[8] in which they were designated PS2 and B25/75, respectively.

B. Method. Small-angle X-ray scattering measurements were performed with a Kratky camera, which was modified[9] and fitted with a Tennelec one-dimensional position-sensitive detector. It was operated with Ni-filtered Cu radiation from a Philips XRG3100 generator operating at 45 kV and 35 mA. The intensity data, collected in a multichannel analyzer, were transferred to a PDP 11/23 laboratory computer, and the correction[9] for the nonuniformity of the detector efficiency along its window length was applied first before other corrections for background, slit smearing, etc. were made. The intensity data were scaled to the absolute unit by comparison with the scattering from a calibrated Lupolen sample[10] kindly supplied by Professor O. Kratky. The correction for the slit-smearing effect was performed by the desmearing algorithms of Glatter[11] and of Strobl.[12]

0024-9297/84/2217-0183$01.50/0